

Structures and mechanical behaviors of $Zr_{55}Cu_{35}Al_{10}$ bulk amorphous alloys at ambient and cryogenic temperatures

Cang Fan,^{1,*} P. K. Liaw,¹ V. Haas,² J. J. Wall,^{1,3} H. Choo,¹ A. Inoue,⁴ and C. T. Liu¹¹*Department of Materials Science & Engineering, The University of Tennessee, Knoxville, Tennessee 37996, USA*²*DaimlerChrysler AG, HPC C320, 70327 Stuttgart-Untertürkheim, Germany*³*LANSCE-LC, Los Alamos National Laboratory, Los Alamos, New Mexico 87544, USA*⁴*Institute for Materials Research, Tohoku University, Sendai, 980-8577, Japan*

(Received 15 March 2006; revised manuscript received 15 May 2006; published 14 July 2006)

Based on a systematic study of pair distribution functions, carried out at cryogenic and ambient temperatures, on as-cast and crystallized ternary Zr-based bulk amorphous alloys (BAAs), we found that the atoms in BAAs are inhomogeneously distributed at a local atomic level. They exist as different clusters with significantly shorter bond lengths than their crystallized counterpart structures—intermetallic compounds, and these structures exist stably in the amorphous state. This results in additional free volume, which is about $\sim 7\%$ larger than that measured by the Archimedes method. The compressive strength measured at ~ 77 K was found to be $\sim 16\%$ larger than that measured at 298 K. In this study, an amorphous structural model is proposed, in which strongly bonded clusters acting as units are randomly distributed and strongly correlated to one another, as the free volume forms between clusters. Simulations with reverse Monte Carlo were performed by combining icosahedral and cubic structures as the initial structures for the BAA. The simulations show results consistent with our model. An attempt has been made to connect the relationship between amorphous structures and their mechanical properties.

DOI: [10.1103/PhysRevB.74.014205](https://doi.org/10.1103/PhysRevB.74.014205)

PACS number(s): 61.43.Dq, 61.43.Bn, 62.20.-x

I. INTRODUCTION

Amorphous alloys, which exhibit no long-range structural periodicity, demonstrate many unique properties, such as ultrahigh strength and very large elastic elongation to failure,^{1,2} low temperature superconductivity,³ and good magnetic properties.^{2,4} The potential for the application of these materials has attracted the attention of scientists for decades. In recent years, significant breakthroughs in the field have allowed the improvement of several aspects that have historically limited their application. For example, process cooling rates have decreased several orders of magnitude, from $\sim 10^6$ K/s (Ref. 5) in 1960, to 10^0 – 10^2 K/s,^{2,6–9} in more recent years. Furthermore, the historically brittle materials can exhibit greatly enhanced plasticity, from less than 1% in monolithic bulk amorphous alloys (BAAs) to 10–20% in amorphous alloy composites, which contain nanoscale or microscale crystallites.^{10–15} While the processing and properties of BAAs have been studied extensively at room and elevated temperatures,^{2,6–23} their local atomic structures and mechanical behavior at cryogenic temperatures remain a mystery.

Structural models of BAAs are typically based on hard-sphere representations, which offer little direct correlation to observed physical properties, such as mechanical behavior.²⁴ A further understanding of local atomic structure in BAAs is critical to developing and manufacturing the next generation of glass forming alloys. As such, the correlation between local atomic structure and observed physical properties in BAAs seems a much anticipated evolution of the current state of knowledge.

Pair distribution functions (PDFs) possess useful local atomic pair information, such as distances between central and neighboring atoms and the nature of neighboring atoms, etc. PDFs can be experimentally determined by diffraction

measurements using x rays, neutrons, or electrons, or by the method of extended x-ray absorption fine structure.²⁵ To date, the majority of PDF simulations have been performed on binary systems,^{26–30} while BAAs typically contain three or more elemental constituents. As such, a fundamental understanding of multicomponent BAAs at the atomic level remains an ambiguous, controversial, topic in condensed matter physics.

Previous experiments conducted at a synchrotron x-ray source showed variations in scattering data as a function of position on the BAA samples. This was likely due to small probe size. In order to obtain true *volume average* data representative of the entire bulk amorphous samples, it was determined that neutron scattering was the ideal method for obtaining the PDFs for this study. The very high Q_{\max} of the neutron experiments allowed the resolution of the different lengths of atomic pairs accurately. In contrast to previous work, that deals mostly with the one-dimensional analysis from PDFs, we chose to focus on the three-dimensional atomic configuration reconstructed using the reverse Monte Carlo (RMC) (Ref. 31) method, which produced the excellent fits to the experimental spectra.

II. EXPERIMENT

Samples of $Zr_{55}Cu_{35}Al_{10}$ (compositions in atomic percent), which can be cast into amorphous rods of 5 mm more in diameter, were prepared from high purity raw materials by arc melting under a Ti-gettered Ar atmosphere. The master alloy ingot was melted multiple times and, subsequently, cast into a copper mold to produce cylindrical rods with dimensions of 3 mm in diameter and 75 mm in length. Uniaxial compression tests were conducted on specimens with 6 mm

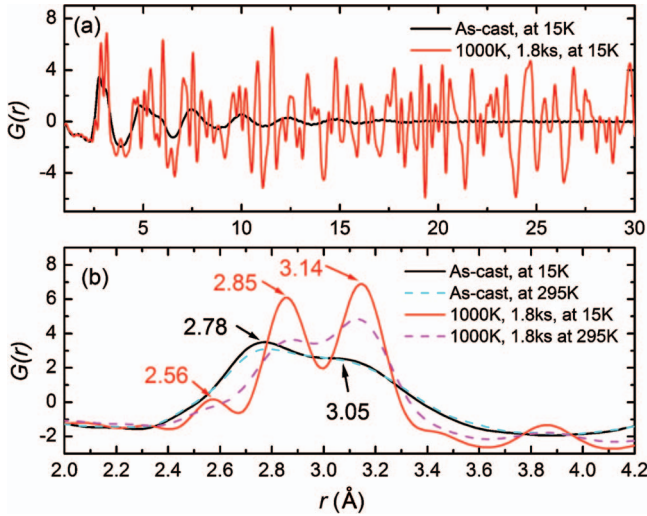


FIG. 1. (Color) (a) Entire image and (b) enlarged area for the nearest peaks of the PDFs, $G(r)$, measured at 298 and 15 K on NPDF for as-cast and crystallized $Zr_{55}Cu_{35}Al_{10}$ BAAs. The annealing was performed for 1.8 ks at 1000 K. The main crystallized phase is $CuZr_2$.

lengths (3 mm diameter), at ambient and cryogenic temperatures, at a strain rate of $1 \times 10^{-3} \text{ s}^{-1}$.

Neutron scattering data for the PDF analyses were collected on the neutron powder diffractometer (NPDF), a high-resolution, total-scattering, powder diffractometer at the Manuel J. Lujan Neutron Scattering Center at the Los Alamos National Laboratory, USA.

PDF is a real-space diffraction analysis method, in which powder diffraction data $I(Q)$ are collected over a wide Q range (up to 51.1 \AA^{-1}), where $Q=4\pi \sin \theta/\lambda$. The PDF $G(r)$ was computed using PDFgetN (Ref. 32) from the Fourier transform of $Q[S(Q)-1]$:

$$G(r_k) = 2/\pi \sum Q_j [S(Q_j) - 1] \sin(Q_j r_k) \Delta Q_j. \quad (1)$$

Modeling was performed by RMC (Ref. 31) using the DISCUS software.^{33,34}

III. RESULTS AND DISCUSSION

Time of flight neutron scattering patterns of as-cast and heat-treated $Zr_{55}Cu_{35}Al_{10}$ BAAs were measured at room temperature and 15 K. PDF analyzes were performed (1) at the different temperatures to investigate the thermal effects on structural states and bonding in the material, and (2) at the different structural states (as-cast and crystallized), which were used to determine the bonding configurations of atomic pairs. Figure 1(a) shows the PDF analysis of the patterns measured at 15 K, $G(r)$ vs r , where r is the distance between pairs. In contrast to the PDFs of annealed (crystallized) materials, which exhibit sharp peaks to large distances, corresponding to structural periodicity, the as-cast structure shows a relatively strong correlation among nearest pairs, quickly becoming diluted and decreasing to zero beyond 16 Å. The nearest pair peaks reveal detailed information about the short-range order, which is of primary importance to under-

stand amorphous structures. Figure 1(b) shows enlarged curves of Fig. 1(a) for the nearest pairs. By using a least squares fitting method, it was determined that peaks around 2.56 and 2.8 Å (error $\pm 0.005 \text{ \AA}$) are mainly due to the contributions of Cu-Cu and Zr-Cu pairs. The peaks around 3.05 Å are from Zr-Al, Zr-Zr, and Zr-Cu pairs. The intensities of the PDF for the as-cast samples at 15 K increased slightly around peak positions of 2.78 and 3.05 Å and narrowed slightly, compared with that at room temperature. On the contrary, the intensity of the PDF for the annealed samples measured at 15 K increased significantly at the positions of 2.56, 2.85, and 3.14 Å as the curve became sharper. It is unlikely that atomic vibrations were the main factor influencing the structure of the amorphous state on the atomic level since the random distributions in amorphous solids keep the atoms fixed quasistatically. The more notable characteristics of the figure are as follows.

(1) The peak values for pairs in the amorphous materials are significantly smaller than those in the annealed materials; 2.78 and 3.05 Å for the amorphous solid, and 2.85 and 3.14 Å for the crystallized solid. From this value, the established density for the local atomic structure of the amorphous solid is $\sim 7\%$ higher than that for the annealed structure. This comes into conflict with their density change, as measured by the Archimedes method on the macroscale, in which the densities for the crystallized solids are about 0.3–3 % higher than the corresponding initial amorphous solids.

(2) Instead of a single PDF peak at the nearest pair position, which would represent a truly random atomic configuration, the PDF of the amorphous solid shows multiple peaks at the nearest pair positions, 2.78 and 3.05 Å. In fact, at 2.56 Å there is a significant degree of peak overlap, indicating that different clusters with different bond lengths exist in the bulk amorphous solid. Similar results of shorter bond lengths in the amorphous state have been found to occur in other Zr-, Cu-, and Mg-based (not presented here), as well as Fe-based³⁵ BAAs. The shorter bond lengths and the different clusters at the local atomic level should have a direct or indirect connection with the glass forming ability and physical properties in BAAs.

The peak widths contain the atom-pair probability distribution, in which thermal and zero-point motion of atoms and any static displacement of the atoms away from ideal lattice sites give rise to a distribution of atom-atom distances, therefore broadening the PDF peaks.²⁵ The influence of thermal vibrations on the PDFs was not significant at 15 K, as compared to room temperature, thus the temperature effect on atomic structures is likely insignificant. To further investigate the difference between the as-cast and crystallized samples, the FWHM (full width at half maximum) of the peaks around 2.8 and 3.05 Å and their change from room temperature to 15 K are listed in Table I. As shown in the table, from room temperature to 15 K, the FWHM of crystallized $CuZr_2$ phase decreased 44% and 30% for the peaks around 2.8 and 3.05 Å, respectively; however, it only reduced 7% and 5% in the amorphous phase for the peak around 2.8 and 3.05 Å, respectively. This implies that atomic pairs bond tightly in the amorphous state. The FWHMs of the amorphous phase are ~ 0.4 and $\sim 0.57 \text{ \AA}$ for the peak around 2.8 and 3.05 Å, respectively. These are two times larger than those of the

TABLE I. FWHM W_{RT} and W_{LT} at room temperature and 15 K, respectively, and the differences δ [$\delta = (W_{LT} - W_{RT})$], and the percentage, δ/W_{RT} (%), for amorphous and crystallized $Zr_{55}Cu_{35}Al_{10}$ BAAs (data collected at NPDF).

	Peak around 2.8 Å				Peak around 3.05 Å			
	W_{RT}	W_{LT}	δ	δ/W_{RT}	W_{LT}	W_{RT}	δ	δ/W_{RT}
Cry.	0.350	0.196	-0.154	-44.0	0.300	0.210	-0.09	-30.0
Amor.	0.430	0.400	-0.03	-7.0	0.604	0.572	-0.032	-5.3

crystallized $CuZr_2$ phase at 15 K, which are ~ 0.2 and ~ 0.21 for the peak around 2.8 and 3.05 Å, respectively. This illustrates that some atom pairs in the amorphous phase have a distribution of bond lengths, both shorter and longer than their crystalline counterpart phase, resulting in broadening of the peaks at both small, and large distances, respectively.

Amorphous solids have lower density than their crystalline counterparts on the macro scale because they contain free volume. If atoms with shorter bond lengths are in compressive stress states, and atoms with longer bond lengths are in tensile stress states, these stresses could be alleviated through the presence of free volume between the atoms. This begets the questions: “why do amorphous phases exhibit negligible thermal vibration?” And “how can local atomic pairs with shorter bond lengths in compressive stress states exist in relative equilibrium with free volume?” To answer these questions, we must assume that (1) the compressive stresses between atoms that are away from their mean positions [on the compressive (left) side of the peak] do not exist to a significant extent, and (2) amorphous phases are extremely inhomogeneously distributed at the local atomic level and are strongly bonded to each other as clusters. In contrast to a distribution of atoms acting as hard spheres, these clusters, with shorter bond lengths, may be assumed to be “hard spheres” in topology modeling. Comparison of the PDFs between the as-cast and structurally relaxed samples shows only very small changes occurring after structural relaxation, after which, not only are the structures relaxed, but the stresses as well.³⁶ This proves the first assumption. To estimate a structural model to understand the second assumption, we constructed a structure that contains both icosahedral and cubic bcc structures using RMC simulation.

The peak value of 2.78 Å of the PDF for the as-cast BAA is close to the calculated PDF peak position of 2.82 Å for a bcc $ZrCu$ intermetallic compound. What, then is the most likely structure that contributes to the peak position at 3.05 Å? It has been argued that the transformation barrier to crystallization in BAAs arises from incompatible local atomic configurations in the liquid and in the crystal, respectively.^{2,6} An icosahedral packing of 20 slightly distorted tetrahedrons is denser than fcc or hcp structures. While the icosahedral packing is incompatible with translational periodicity, it has been demonstrated to be a natural phenomena in undercooled liquid structures.³⁷

It is well known that the mixing enthalpy ΔH_{mix} of a binary regular solution of A and B atoms can be calculated from the enthalpy of pure A and pure B ,³⁸ i.e.,

$$\Delta H_{mix} = \Omega_{AB} X_A X_B, \quad (2)$$

where X_A and X_B the mole fractions of A and B , respectively, in the binary solution and $X_A + X_B = 1$, and

$$\Omega_{AB} = N_a z \epsilon = N_a z [\epsilon_{AB} - (\epsilon_{AA} + \epsilon_{BB})/2], \quad (3)$$

where N_a the Avogadro's number, z the number of bonds per atom, and ϵ the difference between the A - B bond energy (ϵ_{AB}) and the average of the A - A (ϵ_{AA}) and B - B (ϵ_{BB}) bond energies, i.e., $\Omega_{AB} < 0$ indicates that the bond energy of A - B is lower than that of A - A or B - B , namely, the interatomic bond of A - B is more stable than that of A - A or B - B . Usually, we can use ΔH_{mix} to express the interaction between A and B atoms, since it has the relationship with Ω_{AB} as described by Eq. (2).

Using the above theory, the presence of the short-range order domains in the Zr - Cu - Al liquid may be estimated by the negative mixing enthalpy. The mixing enthalpy in Zr - Al is estimated to be -44 kJ/mol being considerably more negative than that of all other atomic pairs in the present alloy (-23 kJ/mol for Zr - Cu , and -0.8 kJ/mol for Cu - Al).³⁹ Thus, Al should have strong attractive interaction with Zr . This may lead to the formation of short-range order (Zr , Al) domains in a liquid state. When the liquid is cooled below the liquidus temperature it enters into a metastable state. If nucleation is suppressed, the liquid is maintained as a metastable phase during the glass transition as the atomic configuration is frozen in the liquid configuration, i.e., the short-range order (Zr , Al) rich domains remain in the amorphous phase. Consequently, if we put an Al atom into the center of an icosahedral array around Zr atoms, we find that the nearest PDF position is at 3.05 Å.

Considering the existence of the bcc $ZrCu$ and icosahedral-like short-range ordering in the BAA, we performed RMC modeling on our experimental data. Unlike crystalline metals, amorphous structures are more complicated and do not have a small, unique unit cell. As such, large numbers of atoms were required in the computer simulation. RMC is a general method of structural modeling based on experimental data and works within constraints, in which the creation of reasonable initial configurations is the key step, and can handle a large number of atoms for modeling. It is useful for aiding the understanding of either the structure itself or of the relationships between local structure and other physical properties.³¹ Based on the above discussion, instead of generating a random homogenous structure at the atomic level, randomly distributed icosahedral plus bcc

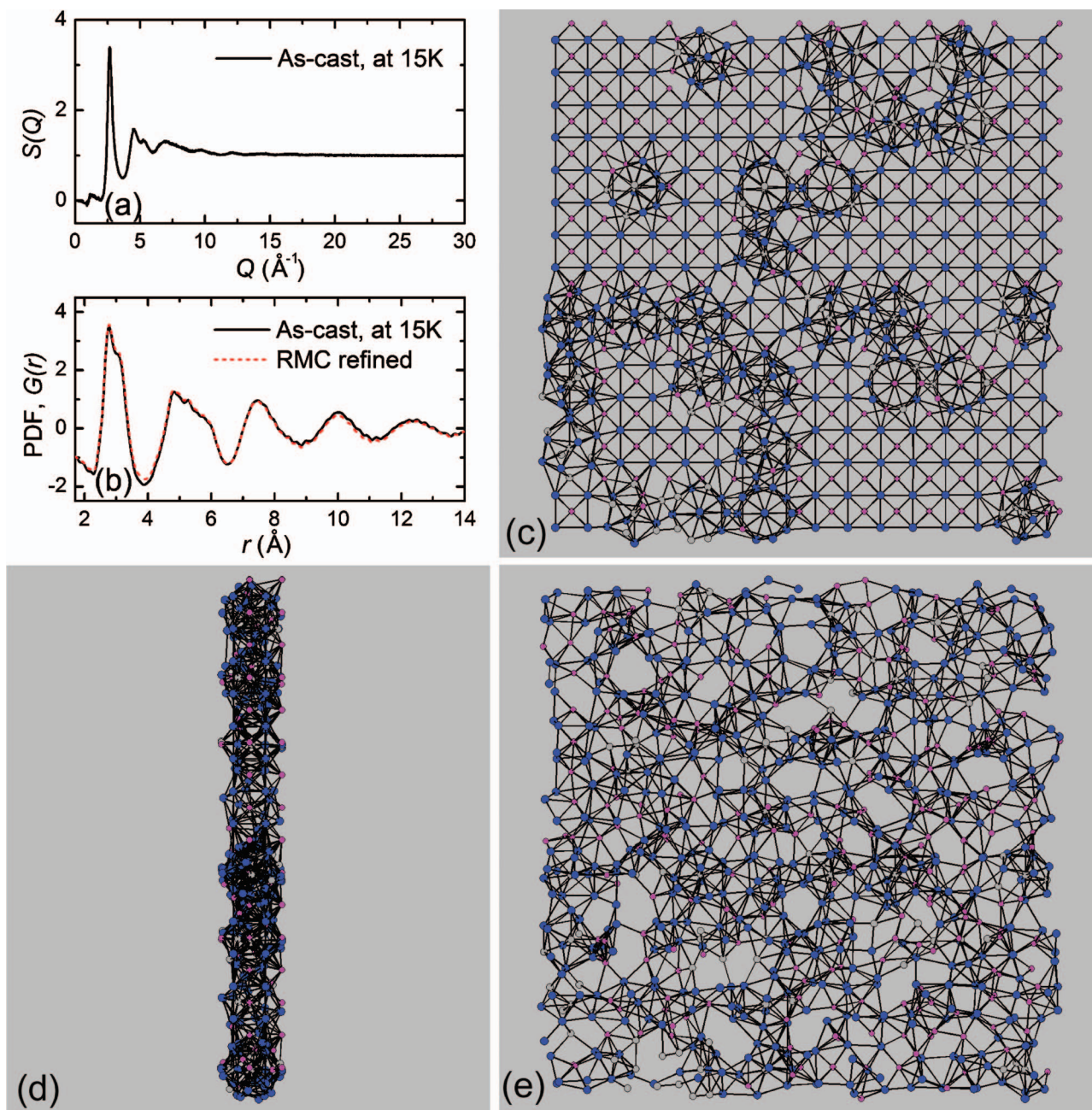


FIG. 2. (Color) (a) and (b) $S(Q)$ vs Q and PDF of as-cast $Zr_{55}Cu_{35}Al_{10}$ BAAs measured at 15 K on NPDF together with that refined by RMC; (c) partial structure with one icosahedral cell thickness [shown in (d)] taken from the initial structure for RMC refinement, consisting of clusters of randomly distributed icosahedral plus bcc structures; (e) the same layer as that shown in (c) after RMC refinement.

clusters were chosen for the initial configurations. The initial configuration consists of 7682 atoms and the icosahedral structures were generated randomly in position and direction (icosahedral structures were randomly rotated during generation) by our own Fortran code. As an example, we present a layer that has one icosahedral cell thickness as shown in Figs. 2(c) and 2(d). The refined curve is shown in Fig. 2(b) along with the $S(Q)$ vs Q diffraction pattern shown in Fig. 2(a). Figure 2(e) shows the refined structure, which is the same layer as shown in Fig. 2(c). After refinement, many bcc and icosahedral structures were deformed, and these structures evolved from their original shapes. Nevertheless, a

number of icosahedral-like structures, with similar original shape or imperfect shapes (in which certain atoms are off from the ideal icosahedral positions), still remain in the refined model. Note that the refined structure shows many clusters existing in the amorphous phase, while large numbers of vacancies appear in the structure, separating the continuity of the strongly bonded pairs into clusters, subsequently forming free volume. Shorter bond lengths in the as-cast samples compared with the crystallized samples exist inside of the clusters, allowing them to exist in relative equilibrium with free volume, which exists between the randomly connected clusters. Since the strongly bonded clusters

have a higher density by $\sim 7\%$ than the crystallized structure, the amount of the free volume in amorphous phase should be $\sim 7\%$ larger than that measured by the Archimedes method.

Based on our analysis and modeling, we propose that structures of BAAs are built by randomly distributed, well correlated clusters, in which atoms are strongly bonded to each other. The combination of the bond properties inside and between these clusters determine the degree of strength and ductility of the materials. The spaces between clusters as free volume may provide room for the translation or rotation of clusters upon applied loading, dictating the deformation characteristics of the material. This model can explain why shear bands, which are the mode of deformation of amorphous alloys, have a defined thickness (~ 20 nm) (Refs. 40 and 41) and propagate with the motion of a plane that contains a relatively large number of atoms. Because no long-range order exists, dislocations cannot form, instead, large cells of free volume provide room for cluster rotation, as shown in Fig. 2(e) (the refined layer is much smaller than 20 nm, but contains larger numbers of vacancies—free volume). If large numbers of clusters fail to cooperatively rotate together, a single cluster cannot rotate to move further. The cooperative rotating clusters form a layer of reconfiguration which deforms amorphous alloys during applied loading. This model can also explain why some amorphous alloys are less brittle than others. As shown above, if the bond lengths of the clusters are close to, or even shorter than, those of their crystallized counterpart intermetallic compounds, the combination of strength and brittleness of the bonding properties in different clusters will govern the strength and ductility of the BAAs, on a macroscopic scale. If the crystallized counterpart intermetallic compounds are less brittle, then the counterpart amorphous alloys may show less brittle properties. If the bond length of the clusters is close to that in their counterpart solution alloys, the amorphous alloys should possess more ductility. For example, we have found that when the intensity of the short bond length near 2.8 \AA (bcc ZrCu like) in PDF decreases and the bond length near 3.05 \AA , which is close to that in solution alloys (Zr-Al and Zr-Pd bonds, when Pd has been added) increases, the plastic deformation after yielding is markedly increased. This is likely to be one of the main reasons that the Pd containing amorphous alloys have increased ductility.^{10,13} By studying the PDFs, it is possible to define the bond lengths and properties of the local atomic clusters, which provides an atomistic basis for describing the mechanical properties of amorphous alloys.

The change in mechanical behavior of the materials is of note as the PDF varies from ambient to cryogenic temperatures. Figure 3 shows the stress-strain curves of the as-cast $\text{Zr}_{55}\text{Cu}_{35}\text{Al}_{10}$ BAAs. The materials show comparable plastic deformation ($\epsilon_p=0.1\text{--}0.7\%$) while the strength increased significantly ($\sim 16\%$) when measured at ~ 77 K. From the results shown, it is apparent that the amorphous matrix does not exhibit a ductile to brittle transition temperature when lowered to ~ 77 K. The average fracture strengths are ~ 1740 and ~ 2020 MPa measured at 298 and ~ 77 K, respectively. This change is consistent with the change of the PDFs. The FWHM of the nearest peaks decreased 5–7% when the temperature was lowered from 298 to 15 K. The decrease of the thermal vibrations contributes to the increase of the strength

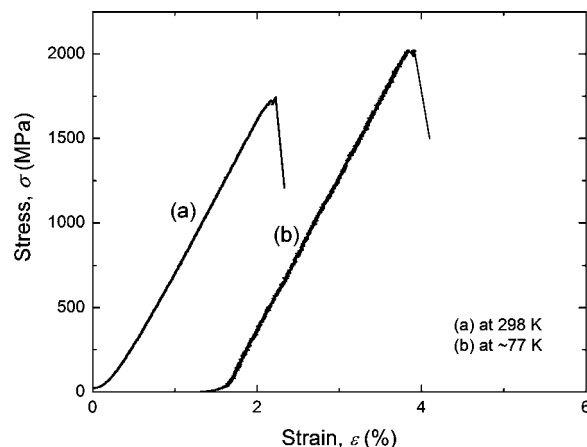


FIG. 3. Stress-strain curves of as-cast $\text{Zr}_{55}\text{Cu}_{35}\text{Al}_{10}$ BAAs measured at 298 and ~ 77 K.

of the BAAs. The essentially unchanged structural characteristics result in comparable plastic deformation between the room and cryogenic temperatures, since the plastic deformation is dominated by highly localized shear bands, which propagate through large numbers of cooperative rotating clusters. From this deformation behavior, where temperatures rise inside shear bands, is another important factor that dictates the deformation behavior. It has been reported that in the center of shear bands, the temperature can rise over 3100 K from ambient temperature,^{42,43} which is much higher than the melting temperature (normally ~ 1100 K) of most BAAs, thus resulting in shear softening. We also found that a molten surface exists on a shear failed Ta wire (Ta melting temperature: 3293 K), which is 0.5 mm in diameter and cast into the center of 3 mm in diameter amorphous rod samples. As the testing temperature was about 220 K lower than ambient temperature, it is likely not sufficient to influence shear-band operation.

IV. CONCLUSION

Based on a systematic study of pair distribution functions, carried out at cryogenic and ambient temperatures, on as-cast and crystallized ternary Zr-based BAAs, we found that the atoms in BAAs are inhomogeneously distributed at a local atomic level. They exist as localized clusters with significantly shorter bond lengths than their crystallized structures—intermetallic compounds, and these structures exist stably in the amorphous state. This results in additional free volume, which is about $\sim 7\%$ larger than that measured by the Archimedes method. The compressive strength measured at ~ 77 K was found to be $\sim 16\%$ larger than that measured at 298 K. In this study, an amorphous structural model is proposed, in which, strongly bonded clusters acting as units are randomly distributed and strongly correlated to one another as free volume forms between clusters. Simulations with RMC were performed by combining icosahedral and cubic structures as the initial structures for the $\text{Zr}_{55}\text{Cu}_{35}\text{Al}_{10}$ BAA. The simulations show results consistent with our model. It has been demonstrated that the relationship between amorphous structures and their mechanical

properties can be described using this model. The combination of the bond properties inside and between these clusters dominates the strength and ductility of the amorphous alloys. The free volume between the clusters provides room for a rotation of the clusters. This cooperative rotation of clusters forms shear bands during applied loading.

ACKNOWLEDGMENTS

The authors would like to acknowledge valuable discussions with T. Egami, S.J.L. Billinge, and T. Hufnagel. This

work was supported by the National Science Foundation International Materials Institutes (IMI) Program under Grant No. DMR-0231320. This work has benefited from the use of NPDF at the Lujan Center at Los Alamos Neutron Science Center, funded by DOE Office of Basic Energy Sciences and Los Alamos National Laboratory funded by The Department of Energy under Contract No. W-7405-ENG-36 (the upgrade of NPDF has been funded by NSF through Grant No. DMR 00-76488). The author C.T. Liu is supported by the Division of Materials Science and Engineering, Office of Basic Energy Sciences, US Department of Energy, under Contract No. DE-AC05-00OR-22725 with UT-Battelle, LLC.

*Email address: cfan@utk.edu

- ¹W. L. Johnson, *MRS Bull.* **24**, 42 (1999).
- ²A. Inoue, *Uetikon-Zuerich* (Trans Tech Publications, Switzerland, 1998).
- ³Y. Li, H. Y. Bai, P. Wen, Z. X. Liu, and Z. F. Zhao, *J. Phys.: Condens. Matter* **15**, 4809 (2003).
- ⁴K. Yamauchi, Y. Yoshizawa, and S. Nakajima, *Mater. Sci. Eng.* **99**, 95 (1988).
- ⁵W. Klement, R. Willens, and P. Duwez, *Nature (London)* **187**, 869 (1960).
- ⁶W. L. Johnson, *Intermetallic Compounds*, (Wiley, New York, 1994), Vol. 1, p. 687.
- ⁷Z. P. Lu, C. T. Liu, and J. R. Thompson, and W. D. Pouter, *Phys. Rev. Lett.* **92**, 245503 (2004).
- ⁸V. Ponnambalam, S. J. Poon, and G. J. Shiflet, *J. Mater. Res.* **19**, 1320 (2004).
- ⁹H. Ma, E. Ma, and J. Xu, *J. Mater. Res.* **18**, 2288 (2003).
- ¹⁰C. Fan, A. Takeuchi, and A. Inoue, *Mater. Trans., JIM* **40**, 42 (1999).
- ¹¹J. Eckert, U. Kuhn, J. Das, S. Scudino, and N. Radtke, *Adv. Eng. Mater.* **7**, 587 (2005).
- ¹²C. Fan, C. Li, A. Inoue, and V. Haas, *Phys. Rev. B* **61**, R3761 (2000).
- ¹³C. Fan and A. Inoue, *Appl. Phys. Lett.* **77**, 46 (2000).
- ¹⁴C. C. Hays, C. P. Kim, and W. L. Johnson, *Phys. Rev. Lett.* **84**, 2901 (2000).
- ¹⁵C. Fan, R. T. Ott, and T. C. Hufnagel, *Appl. Phys. Lett.* **81**, 1020 (2002).
- ¹⁶C. Fan and A. Inoue, *Mater. Trans., JIM* **38**, 1040 (1997).
- ¹⁷C. Fan, D. V. Louzguine, C. F. Li, and A. Inoue, *Appl. Phys. Lett.* **75**, 340 (1999).
- ¹⁸J. Eckert, M. Seidel, A. Kubler, U. Klement, and L. Schultz, *Scr. Mater.* **38**, 595 (1998).
- ¹⁹C. Fan, H. Choo, and P. K. Liaw, *Scr. Mater.* **53**, 1407 (2005).
- ²⁰T. G. Nieh, T. Mukai, C. T. Liu, and J. Wadsworth, *Scr. Mater.* **40**, 1021 (1999).
- ²¹T. G. Nieh, J. Wadsworth, C. T. Liu, T. Ohkubo, and Y. Hirotsu, *Acta Mater.* **49**, 2887 (2001).
- ²²P. Wesseling, T. G. Nieh, W. H. Wang, and J. J. Lewandowski, *Scr. Mater.* **51**, 151 (2004).
- ²³M. L. Morrison, R. A. Buchanan, A. Peker, W. H. Peter, J. A. Horton, and P. K. Liaw, *Intermetallics* **12**, 1177 (2004).
- ²⁴S. M. Allen and E. L. Thomas, *The Structure of Materials* (John Wiley & Sons, Inc., New York, 1999).
- ²⁵T. Egami and S. J. L. Billinge, *Underneath the Bragg Peaks: Structural Analysis of Complex Materials* (Pergamon Press, Oxford, 2003).
- ²⁶Y. Waseda, *The Structure of Non-Crystalline Materials, Liquids and Amorphous Solids* (McGraw-Hill, New York 1980).
- ²⁷H. W. Sheng, J. H. He, and E. Ma, *Phys. Rev. B* **65**, 184203 (2002).
- ²⁸K. Kohary, V. M. Burlakov, D. G. Pettifor, and D. Nguyen-Manh, *Phys. Rev. B* **71**, 184203 (2005).
- ²⁹S. Gruner, I. Kaban, R. Kleinhempel, W. Hoyer, P. Jovari, and R. G. Delaplane, *J. Non-Cryst. Solids* **351**, 3490 (2004).
- ³⁰H. W. Sheng, W. K. Luo, F. M. Alamgir, J. M. Bai, and E. Ma, *Nature (London)* **439**, 419 (2006).
- ³¹R. L. McGreevy, *J. Phys.: Condens. Matter* **13**, 877 (2001).
- ³²P. F. Peterson, M. Gutmann, and Th. Proffen, and S. J. L. Billinge, *J. Appl. Crystallogr.* **33**, 1192 (2000).
- ³³Th. Proffen and R. B. Neder, *J. Appl. Crystallogr.* **30**, 171 (1997).
- ³⁴Th. Proffen and R. B. Neder, *J. Appl. Crystallogr.* **32**, 838 (1999).
- ³⁵T. Ohkubo, H. Kai, A. Makino, and Y. Hirotsu, *Mater. Sci. Eng., A* **312**, 274 (2001).
- ³⁶T. Egami, *Ann. N.Y. Acad. Sci.* **371**, 238 (1981).
- ³⁷K. F. Kelton, *J. Non-Cryst. Solids* **334**, 253 (2004).
- ³⁸D. A. Porter and K. E. Easterling, *Phase Transformations in Metals and Alloys* (Reinhold, Van Nostrand, 1981).
- ³⁹F. R. de Boer, R. Boom, W. C. M. Mattens, A. R. Miedena, and A. K. Niessen, *Cohesion in Metals* (Elsevier Science Publishers, Amsterdam, 1989).
- ⁴⁰E. Pekarskaya, C. P. Kim, and W. L. Johnson, *J. Mater. Res.* **16**, 2513 (2001).
- ⁴¹D. E. Polk and D. Turnbull, *Acta Metall.* **20**, 493 (1972).
- ⁴²J. J. Lewandowski and A. L. Greer, *Nat. Mater.* **5**, 15 (2006).
- ⁴³C. Fan, H. Li, L. J. Kecskes, K. Tao, H. Choo, P. K. Liaw, and C. T. Liu, *Phys. Rev. Lett.* **96**, 145506 (2006).